Parameter optimization for non-local de-noising using Elite GA

Aksam Iftikhar, Saima Rathore, Abdul Jalil
Department of Computer and Information Sciences,
Pakistan Institute of Engineering and Applied Sciences,
Islamabad, Pakistan.
e-mail: aksam.iftikhar@gmail.com, saimarathore_2k6@yahoo.com, jalil@pieas.edu.pk

***Abstract*—Non-local means de-noising is a simple but effective image restoration method. It exploits usual redundancy found in real-life images. It computes similarity between patches of pixels, in a non-local window, instead of pixels themselves. This similarity measure defines participation/weight of each pixel in the de-noising process. In this research study, non-local means de-noising has been applied to noisy synthetic and brain MR images by optimizing its parameters through Genetic Algorithm. Elite Genetic Algorithm, a novel idea, has also been proposed to optimize several parameters of the non-local framework. It works in a hierarchical structure i.e. K Primary GAs and one Secondary GA. Each Primary GA evolves with independent population and gives rise to n_k elite chromosomes after t generations, which collectively serve as population of Secondary GA. Evolution with Elite GA results in improved speed of convergence as Secondary GA starts its evolution with more fit chromosomes instead of randomly generated population. These elite chromosomes are expected to be better solutions, thus have higher probability to approach global minima/maxima in no time. Algorithm has been tested on the said images and improved convergence rate has been observed for Elite GA. Moreover, the individuals selected by Elite GA are as fit as traditional GA as verified by PSNR and RMSE results.**

Keywords – non-local; de-noising; genetic algorithm; brain MRI;

I. INTRODUCTION

Image de-noising is a vital image restoration process, which aims to remove noise in order to restore better quality image. Images in real life may contain noise of several types which degrade the image quality. The degradation is proportional to the amount of noise present in the image. Such a degraded image is not suitable for subsequent processing. Therefore, it is essential to remove, or at least reduce, the noise present in the image. The process of removing noise in order to restore better quality image is termed as image de-noising. Researchers have put considerable efforts in this regard and efficient noise removal is still an open issue of research.

Several approaches have been proposed to attack the image de-noising problem. The earliest in timeline of these approaches are local neighborhood based image de-noising [1]. A local neighborhood based image de-noising technique employs information of neighboring pixels of a noisy pixel in order to restore its value. Usually, a simple averaging of neighboring pixels is performed to restore original pixel. Other sophisticated approaches use weighting of neighboring pixels, based on some predetermined characteristic, to yield better image de-noising [2]. Local neighborhood based approaches produce effective de-noising but they introduce blurring of edges and remove image detail - an undesirable characteristic.

Non-local image de-noising, first introduced by Buades et al. [3], forms another category of image de-noising techniques which exploit non-local information in an image. It has been used widely in many application for effective image de-noising [4-7]. The motivation of non-local neighborhood based approaches is that images in real life contain a lot of redundancy which can be exploited to remove noise from the image [3]. The term *non-local* was originally used as antonym of *local* in order to designate that the exploited information does not lie in a local neighborhood necessarily. Rather, the information in whole image (ideally) can be exploited in the process of de-noising. The set of neighbors of a pixel in a non local approach are referred to as a patch. A noisy pixel is updated based on spatial similarity of its patch to patch of another pixel in the whole image ideally, and in a window of particular size practically. The size of window is an important parameter which needs to be addressed empirically. However, adaptive window size has also been proposed [20]. A detailed description to the non-local image de-noising will be provided in Section II. Non-local based approaches yield better performance than local neighborhood based approaches. But, they are computationally intensive as comparing every patch in the image to every other patch was not feasible. So, several improvements, in terms of both efficiency and effectiveness, to the basic non-local based image de-noising approach have been proposed [8-12]. These proposed techniques not only reduced the computational burden but also improved the de-noising capability. Other popular image de-noising approaches are anisotropic diffusion filtering [13, 14], total variation minimization based methods [15, 16], wavelet based de-noising [17, 18], Wiener filtering [19] etc.

The performance of non-local based image de-noising is heavily dependent on a few parameters namely the patch size, search window size and the tradeoff parameter denoted. Finding a suitable set of parameters generally requires an exhaustive search for allowable ranges of these parameters, which is infeasible for practical applications. Consequently, researchers have empirically found parameter values within a limited range with certain approximations [4, 5]. But, compromising the parameters range or approximating their values affects the performance of the algorithm and may produce inferior de-noising results. In this work, we have

978-1-4673-2252-2/12/$31.00 ©2012 IEEE

employed a Genetic Algorithm (GA) based optimization to search for optimized set of parameters in the search space. GA strives to minimize an objective value by simulating the natural phenomenon of evolution and employing certain genetic operators. It evaluates a set of problem parameters combinations which form the individuals of its population. Due to such diverse population and powerful genetic operators, GA does not get stuck into local minima and produces optimum result. We have optimized the parameters of non-local means algorithm for application to synthetic and real brain MR images using GA. The objective value for GA is Peak Signal-to-Noise Ratio (PSNR). De-noising of brain MR images has been an active area of research because success of this step alleviates the problems of subsequent stages of processing these images e.g. image segmentation and classification. Thus, de-noising brain MR images indirectly helps in applications such as 3D brain reconstruction, disease diagnosis and monitoring etc. Finally, a novel variation of the traditional GA, termed as Elite GA (EGA), is proposed. It is similar in concept to GA, but strives to accelerate the GA search by starting its evolution with more fit individuals. Elite GA will be described in detail in Section II.

The remainder of this paper is organized as follows. Section 2 describes the proposed scheme. Section 3 describes the quantitative measures used for performance comparison whereas Section 4 presents the experimental results. Finally, Section 5 concludes the paper.

II. PROPOSED SCHEME

In this section, we introduce various elements involved in the proposed scheme for de-noising using non-local means algorithm. First of all, a comprehensive introduction to the non-local de-noising approach is presented in order to get acquaintance with several parameters of this method. Second, we propose to obtain optimal values of these parameters using a Genetic Algorithm (GA) based evolution. Third, a novel variant of conventional GA is proposed. This variant of conventional GA is named as Elite GA (EGA) pertaining to the way it works. These three elements of the proposed scheme are described in following subsections.

A. Non-local de-noising

Given an input image I_{in}, non-local image de-noising computes the output image pixels as a weighted sum of the pixels in a certain non-local neighborhood. This is expressed as follows [3].

$$I_{out}(i) = \sum_{j \in N_i} w(i,j) I_{in}(j) \quad (1)$$

where *w(i, j)* is the similarity between patches of pixels *i* and *j*, denoted by P_i and P_j. Let us denote the size of patch, an important parameter of the algorithm, by R_{sim}. Input image pixel is denoted by $I_{in}(j)$ and $I_{out}(j)$ denotes the corresponding output image pixel. N_i is the non-local window of size R_{search} around pixel *i*, within which the weights *w(i, j)* are computed for pixel *i* against all other pixels *j* in the search window. The weight *w(i, j)* is computed by following expression [3].

$$w(i,j) = \frac{1}{Z(i)} e^{-\frac{\|v(N_i)-v(N_j)\|_{2,a}^2}{h^2}} \quad (2)$$

$$Z(i) = \sum_{j \in N_i} e^{-\frac{\|v(N_i)-v(N_j)\|_{2,a}^2}{h^2}} \quad (3)$$

Where *Z(i)* is a normalization constant. The vector $\boldsymbol{v(P_i)}$ contains the gray level profile of pixels of Patch P_i. The parameter *h* is a tradeoff parameter. It controls the balance between the amount of noise removal and image smoothing. A higher value of *h* removes more noise but induces relatively more blurring and vice versa. The Euclidean norm computed in Eq. 3 computes the distance between P_i and P_j. It is computed as in following expression.

$$\| v(P_i) - v(P_j) \|_2^2 = \sum_{p=1}^{|Pi|} (v^{(p)}(P_i) - v^{(p)}(P_j))^2 \quad (4)$$

Where $v^{(p)}(P_i)$ represents the p^{th} component of vector $\boldsymbol{v(P_i)}$ and $|P_i|$ is the number of elements in vector P_i.

B. Genetic Algorithm

The non-local de-noising method involves 3 critical parameters. The performance of the algorithm is dependent on values selected for these parameters. We have employed a Genetic Algorithm based evolution to find such optimal values for several parameters of non-local de-noising which could maximize nonlocal de-noising capability of the system. Following are the three parameters of non-local de-noising method.

- Search Window Size (R_{search}): It is size of the bounding window around a pixel within which similarity is computed amongst patches of different pixels and patch of central pixel.
- Patch/Similarity Window Size (R_{sim}): It is size of the patch of a particular pixel. The patch size R_{sim} must always be less than or equal to R_{search}.
- Smoothing Parameter (h): This parameter maintains a tradeoff between image smoothness and de-noising. An optimal value of h is required in order to obtain a de-noised image with enough detail present in the image.

Both R_{search} and R_{sim} are specified as radius of corresponding window, i.e. for R_{sim} = 2, actual size of square patch/similarity window will be 5×5 (2*2+1 =5) for 2D images. The 3 parameters, described above, form the individuals of the GA which we employed for finding optimal values of these parameters.

C. Elite Genetic Algorithm

Introducing genetic algorithm for parameter optimization of a given dataset, usually, is a computationally expensive process. Convergence rate can be quite low i.e. it may take a large number of iterations to converge to the parameters which maximize/minimize the objective value. An early, but effective, convergence is always desirable. Particularly, when the objective function is computationally very costly to compute, a delayed convergence of GA adds up to the overall

cost of optimization. In order to alleviate this feature of GA, Elite Genetic Algorithm (EGA) is proposed.

In EGA, multiple GA's are involved in the evolution process. It seems reasonable to divide these GAs into two distinguishing categories. First, a Primary GA (PGA) refers to a temporary GA which is allowed to run only for a predetermined number of generations. Multiple PGAs are involved in an EGA. These PGAs serve as population feeders for Secondary GA (SGA) - the other category of GA in an EGA. Specifically, top N individuals are selected each PGA and all these elites are fed to the SGA to yield its population. These elites, from PGAs, are more fit individuals than randomly selected individuals in conventional GA and are already close to minima of the search space. Hence, it is quite reasonable to assume that EGA can quickly converge and find optimal values of parameters. A graphical illustration of EGA working is presented in Figure 1.

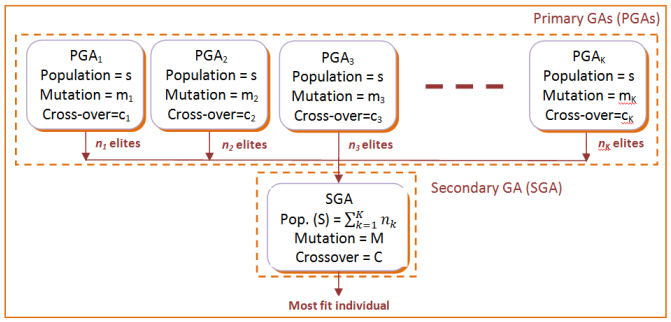

Figure 1. Layout of an Elite GA

Figure 1 shows that there are total K number of Primary GAs and 1 Secondary GA. PGA_k represents the k^{th} Primary GA and each Primary GA can have its own mutation and crossover rate denoted by m_k and c_k, respectively. For simplicity and without loss of generality, we assume $m_k=m$ and $c_k=c$ for all k, i.e. constant mutation and crossover rates are assumed for all PGAs. The elites selected from each PGA are represented by n_k. Again, for simplicity, we assume $n_k=n$ for all k. In Secondary GA, M and C represent the mutation and crossover rates. The population size, denoted by S, is computed as $S=\sum_{k=1}^{K} n_k$. In our case, S can simply be computed as $S=K\times n_k$,due to the assumption that $n_k=n$ for all k.

Elite GA has been employed to optimize several parameters of the non-local de-noising approach in order to improve the convergence rate as compared to conventional GA. The parameters to be optimized are the same as already discussed. More details on EGA for parameter optimization will be provided in Section IV.

III. Performance Evaluation Parameters

Amongst several performance evaluation parameters, we have chosen Peak Signal-to-Noise Ratio (PSNR), and Root Mean Square Error (RMSE) for performance evaluation. These parameters are very commonly used to assess the performance of a de-noising algorithm. They provide overall quantitative measures for an image, which dictate how well a de-noising algorithm has performed in restoring the noisy pixel values.

A. Peak Signal-to-Noise Ratio(PSNR)

PSNR is ratio between the maximum possible power of a signal and power of noise level that corrupts the signal. It provides a measure how much noise is present in the image, and is usually measured in logarithmic decibel (dB) scale. A higher value of PSNR represents better de-noising performance. It is computed by following expression.

$$PSNR = 10\log_{10}(R^2 / MSE)$$

$$MSE = \frac{\sum_{m,n}[I_1(m,n) - I_2(m,n)]^2}{M \times N} \quad (5)$$

Where I_1 *and* I_2 represent original and de-noised images respectively. M and N depict rows and columns of given images, whereas R represents maximum possible gray level present in the image.

B. Root Mean Square Error (RMSE)

RMSE reflects how much results deviate from expected value. It is the square root of sum of square of differences in image intensity values. It can be used as a measure of deviation of restored image from the original image. A lower value of RMSE is desirable as it represents better de-noising performance. It is computed by the following expression.

$$RMSE = \sqrt{\frac{\sum_{m,n}[I_1(m,n) - I_2(m,n)]^2}{M \times N}} \quad (6)$$

Where I_1, I_2 , M and N are same as in Equation (1).

IV. Experimental Results

Experiments have been conducted with real and synthetic brain MR images. Synthetic images were obtained from simulated brain database BrainWeb, whereas real brain images were acquired from Internet Brain Segmentation Repository (IBSR). Synthetic and real brain images have spatial resolution of 169x205 and 256x256, respectively. Synthetic images were experimented in axial view orientation whereas real images were experimented in coronal view orientation. The images in IBSR database are complete head MR images, but region of interest (brain) was extracted prior to applying the de-noising and GA based evolution.

Initially, images of different noise level (=10,15,20) were de-noised using h=1.2σ, R_{sim} = 2 and R_{search} = 5. These parameter values were suggested by authors in previous studies [4]. We will refer to these values as empirical parameter values throughout the rest of paper as these parameters values were empirically found by authors without adopting any proper search mechanism. Hence, the search space is not explored exhaustively. So, there is surely room for further improvement in de-noising results by adopting some search method to obtain more suitable parameter values. We have employed genetic algorithm for such parameter optimization. Values of several variables of GA are listed in Table I. It has been observed that for given images, GA converges well before 50 iterations. So GA, with given settings, was allowed to evolve for a maximum of 50 iterations and minimized objective value (PSNR) was found to obtain the corresponding optimal individual.

The newly proposed variant of GA, called EGA, was also applied on images to obtain optimal values of search parameters. The intention behind introducing EGA was to accelerate the search process and obtain a better convergence rate. As EGA begins its evolution with more fit individuals, an anticipation of faster convergence is quite reasonable. Values of several variables of SGA and multiple PGAs are listed in Table I.

TABLE I. VARIABLE VALUES OF GA AND EGA

Parameter Name	EGA		GA
	PGA	*SGA*	
Number of GA's	05	01	01
Initial Population Size	30	5x6=30	30
Max. Number of iterations	01	50	50
Crossover	0.8	0.8	0.8
Elites selected from each GA	06	-	-
Fitness function	PSNR	PSNR	PSNR

We have obtained several performance results by applying NLM algorithm with parameters suggested by [4], and with parameters obtained by evolving GA and EGA using variable values listed in Table I. In particular, optimal values using GA and EGA, and corresponding PSNR and RMSE values are obtained for the aforementioned approaches. Convergence rate is compared for GA and EGA in terms of number of iterations. Moreover, visual results of de-noising using aforesaid approaches are also obtained.

Table II demonstrates parameter values for real and synthetic brain images. For each image type, parameters were optimized using both GA and EGA. Table II also demonstrates parameter values for NLM. Values are separately calculated for images of different standard deviations. Each entry in Table II is a 3-tuple value that corresponds to R_{sim} , R_{search} and h respectively. For example, 2,5,12 represents $R_{sim} = 2$, $R_{search} = 5$ and $h = 12$.

TABLE II. OPTIMAL VALUES OF SYSTEM PARAMETERS FOR NLM, AND VALUES CALCULATED BY GA AND EGA FOR DIFFERENT IMAGE CATEGORIES

	Synthetic Images			Brain Images		
	NLM	*GA*	*EGA*	*NLM*	*GA*	*EGA*
=10	2,5,12	5,17,10	5,17,10	2,5,12	1,10,7	1,10,7
=15	2,5,18	2,19,10	2,19,10	2,5,18	2,6,13	2,6,13
=20	2,5,24	9,15,16	9,15,16	2,5,24	2,6,18	2,6,18

PSNR was used as fitness value for individuals of GA. The problem of maximizing the PSNR is posed as a minimization problem by negating the PSNR value and then evolving the GA for minimizing the negative PSNR values. This is the reason that negative values appear in graphs presented later in the paper. PSNR and RMSE values corresponding to parameters values listed in Table II are illustrated in Table III. This table provides an insight to quantitatively compare the performance of selected parameters.

Table III presents PSNR and RMSE values obtained respectively for NLM using empirical parameters, for GA and EGA using parameters listed in Table II. The noisy image PSNR and RMSE is computed prior to applying de-noising to the corresponding images. Significantly improved PSNR and RMSE values have been obtained using parameters selected by GA or EGA as compared to empirical parameters for NLM de-noising. Parameters selected both by GA and EGA, and hence resultant performance measures, are similar. This verifies that EGA is as effective as traditional GA in finding optimal individuals. However, EGA results in improved convergence rate as compared to GA in many cases. This can be observed from Table IV, which presents number of iterations taken by GA and EGA before convergence.

TABLE III. PSNR VALUES COMPUTED USING OPTIMIZED PARAMETERS

Noise Variance	Performance measure	Noisy	NLM	GA	EGA
Real Brain Images					
= 10	*PSNR*	19.4695	30.7816	**33.0482**	**33.0482**
	RMSE	10.0025	05.1395	**04.8751**	**04.8751**
= 15	*PSNR*	17.7641	29.3342	**30.6498**	**30.6498**
	RMSE	14.8101	07.0864	**06.4239**	**06.4239**
= 20	*PSNR*	15.7883	28.0754	**28.7061**	**28.7061**
	RMSE	20.0914	08.7777	**08.0387**	**08.0387**
Synthetic Brain Images					
= 10	*PSNR*	21.7084	33.1220	**35.8739**	**35.8739**
	RMSE	10.0614	04.3239	**03.7739**	**03.7739**
= 15	*PSNR*	18.5588	29.8196	**32.8030**	**32.8030**
	RMSE	14.8672	06.4840	**05.2815**	**05.2815**
= 20	*PSNR*	17.3390	28.8281	**31.6690**	**31.6690**
	RMSE	20.0751	09.0491	**06.2915**	**06.2915**

Experiments revealed that EGA converged in lesser number of iterations as compared to GA in most of the cases. Iterations of GA are the number of generations it evolved before convergence. However, in case of EGA, iterations are calculated by adding individual generations taken by PGAs (1 in this case) and SGA. Number of iterations elapsed in different scenarios are given in Table IV.

TABLE IV. COMPARISON OF CONVERGENCE RATE OF SIMPLE GA AND ELITE GA

	Synthetic Images				Real Brain Images			
	Simple GA	*Elite GA*			*Simple GA*	*EGA*		
		PGA	*EGA*	*Total*		*PGA*	*EGA*	*Total*
=10	32	5	21	**26**	33	5	28	**33**
=15	21	5	16	**21**	37	5	21	**26**
=20	21	5	16	**21**	33	5	22	**27**

Table IV demonstrates that in most of the cases, EGA converges in lesser number of iterations. There are a few cases where number of iterations is similar however percentage of such cases is quite small. Convergence graphs of GA and EGA are given in Figure 2 and 3 to demonstrate the convergence pattern of EGA and GA.

Figure 4 presents an example of a noisy and corresponding restored real brain MR images using non-local means (NLM) with empirical parameters and GA/EGA. Original image is presented in Figure 4 (a) for visual comparison with restored versions of the image. It can be observed from Figure 4 (c, d) that both NLM with empirical parameters and GA/EGA selected parameters were able to remove substantial noise from the noisy image shown in Figure 4 (b). However, in order to appreciate the supremacy of GA/EGA selected parameters, a zoomed version of patches of original, NLM and GA/EGA de-noised images are presented in Figure 5. The selected patch is highlighted by a square in Figure 4 (a). From Figure 5, it can be observed that image de-noised using parameters selected by GA/EGA preserves more detail while minimizing the amount

of noise. Whereas, image de-noised using empirical parameters is a bit smoothed out version of original image. Particularly, the area inside the CSF matter in the patch is quite smoothed out as compared to GA/EGA patch.

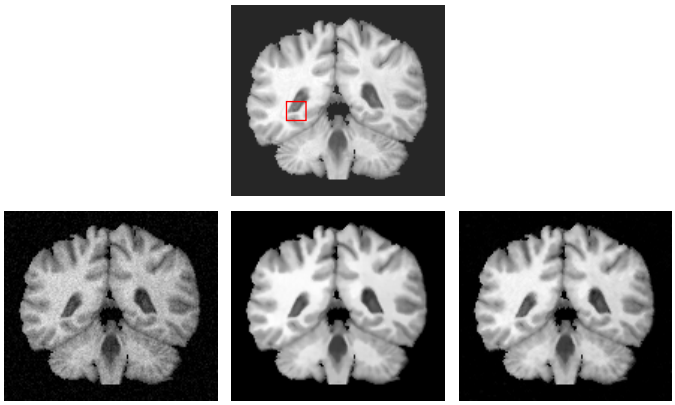

Figure 4. Real Brain MR images, Top row: (a) Original image, Bottom row (left to right): (b) Noisy image (□=10), (c) De-noised image using empirical parameters (d) De-noised image using GA/EGA selected parameters

Figure 5. Selected zoomed patch of Figure 4, (a) Original image patch, (b) Patch of image de-noised using empirical parameters, (c) Patch of image de-noised using GA/EGA selected parameters

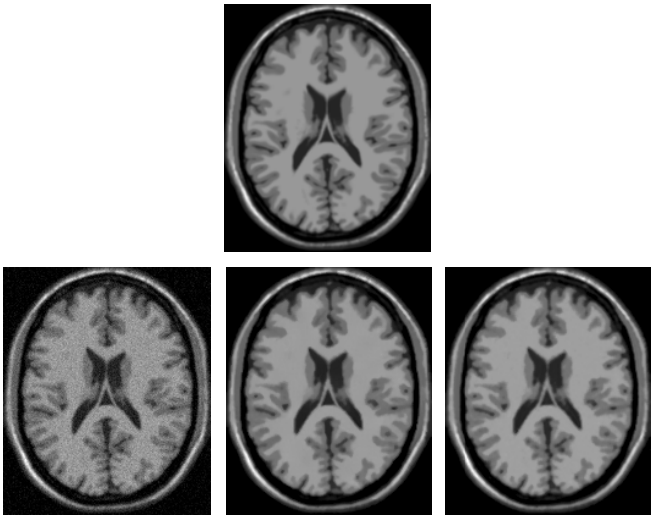

Figure 6. Real Brain MR images, Top row: (a) Original image, Bottom row (left to right): (b) Noisy image (□=10), (c) De-noised image using empirical parameters (d) De-noised image using GA/EGA selected parameters

Similar to Figure 4, the images shown in Figure 6 present different versions of a synthetic brain MR image. It can be seen clearly from Figure 4 that the proposed GA/EGA based parameters are quite effective in de-noising the image. The proposed GA/EGA based parameters also produce better de-noising than empirical parameters which is evident from the PSNR values computed in Table III. Moreover, a careful visual inspection can also verify the superiority of GA/EGA based approach. Hence, it can be quite rationally concluded that the set of parameter values proposed by GA/EGA are more effective in de-noising brain MR images than empirical parameter values already suggested.

V. CONCLUSION

Non-local means (NLM) de-noising is a patch based image de-noising method which exploits non-local information in order to restore noisy pixel values. It has proven to be an effective de-noising method as compared to several other approaches. However, NLM de-noising performance depends upon several parameters of the algorithm such as patch size (R_{sim}), search window size (R_{search}) and the smoothing parameter (h). These parameters have been empirically adjusted in previous studies, thus the search space for these parameters is not explored to its full potential. In this paper, we have alleviated this issue by employing GA to find optimal parameter values to be used in the NLM de-noising. A new variant of GA, called Elite GA, has also been proposed with an intention to improve on convergence time of traditional GA. Improved PSNR and RMSE values have been observed when images are de-noised using optimal parameter values, selected through GA and EGA. Results also reveal faster convergence of EGA when compared against GA, while it is as effective in finding fit individuals as traditional GA.

This research work can be extended in two possible directions. First, to completely explore the potential of EGA, it can be applied to more complex problems involving more than three variables. In such problems, EGA can even find more fit individual than GA, and at the same time converge in reduced number of iterations. Second, PGAs in EGA employ same variable settings (e.g. crossover rate, mutation rate etc.). We can take full advantage of EGA by employing different variable setting for each PGA. This can provide more diverse population which, in turn, can result in improved convergence rate and more fit optimal parameters.

REFERENCES

[1] A. B. Hamza, P. Luque, J. Martinez, and R. Roman, "Removing noise and preserving details with relaxed median filters," J. Math. Imag. Vision, vol. 11, no. 02, pp. 161–177, 1999.

[2] C. Tomasi, and R. Manduchi, "Bilateral filtering for gray and color images," in Proc. ICCV, pp. 839–846, 1998.

[3] A. Buades, B. Coll, and J. M. Morel, "A review of image de-noising algorithms with a new one," Multiscale Modeling and Simulation, vol. 04, no. 02, pp. 490–530, 2005.

[4] J. V. Manjon, J. C. Caballero, J. J. Lull, G. G. Marti, L. M. Bonmati, and M. Robles, "MRI de-noising using non-local means," Medical Image Analysis, vol. 12, pp. 514–523, 2008.

[5] B. Caldairou, N. Passat, P. A. Habas, C. Studholme, and F. Rousseau, "A non-local fuzzy segmentation method: Application to brain MRI," Pattern Recognition, vol. 44, pp.1916–1927, 2011.

[6] J. V. Manjon, P. Coupe, L. M. Bonmati, D. L. Collins, and M. Robles, "Adaptive non-local means de-noising of MR images with spatially varying noise levels," Journal of Magnetic Resonance Imaging, vol. 31, pp. 192–203, 2010.

[7] P. Coupe, P. Hellier, C. Kervrann, and C. Barillot, "Nonlocal means-based speckle filtering for ultrasound images," IEEE Transactions on Image Processing, vol. 18, no. 10, 2009.

[8] P. Coupe, P. Yger, S. Prima, P. Hellier, C. Kervrann, and C. Barillot, "An optimized blockwise nonlocal means de-noising filter for 3-d magnetic resonance images," IEEE Transactions on Medical Imaging, vol. 27, no. 04, 2008.

[9] A. Rehman, and Z. Wang, "SSIM-based non-local means image de-noising," IEEE International Conference on Image Processing (ICIP11), 2011.

[10] D. V. D. Ville, and M. Kocher, "SURE based non-local means," IEEE Signal Processing Letters, vol. 16, no. 11, 2009.

[11] C. Kervrann, and J. Boulanger, "Optimal spatial adaptation for patch-based image de-noising," IEEE Transactions on Image Processing, vol. 15, no. 10, 2006.

[12] A. T. Vega, V. G. Perez, S. A. Fernandez, and C. F. Westin, "Efficient and robust nonlocal means de-noising of MR data based on salient features matching," Computer Methods and Programs in Biomedicine, vol. 105, pp. 131-144, 2012.

[13] P. Perona, and J. Malik, "Scale space and edge detection using anisotropic diffusion," IEEE Trans. Patt. Anal. Mach. Intell., vol. 12, pp. 629–639, 1990.

[14] L. Alvarez, P. L. Lions, and J. M. Morel, "Image selective smoothing and edge detection by nonlinear diffusion. II," SIAM J. Numer. Anal., vol. 29, pp. 845–866, 1992.

[15] L. Rudin, S. Osher, and E. Fatemi, "Nonlinear total variation based noise removal algorithms," Phys. D, vol. 60, pp. 259–268, 1992.

[16] S. Osher, M. Burger, D. Goldfarb, J. Xu, and W. Yin, "An iterative regularization method for total variation-based image restoration," Multiscale Model. Simul., vol. 04, pp. 460–489, 2005.

[17] D. Donoho, "De-noising by soft-thresholding," IEEE Trans. Inform. Theory, vol. 41, pp. 613–627, 1995.

[18] D. Donoho, and I. Johnstone, "Ideal spatial adaptation via wavelet shrinkage," Biometrika, vol. 81, pp. 425–455, 1994.

[19] L. P. Yaroslavsky, "Digital picture processing. An introduction," Springer-Verlag, 1985.

[20] Charles Kervrann and Jérôme Boulanger, "Optimal spatial adaptation for patch-based image denoising," IEEE Transactions on Image Processing, vol. 15, no. 10, 2006

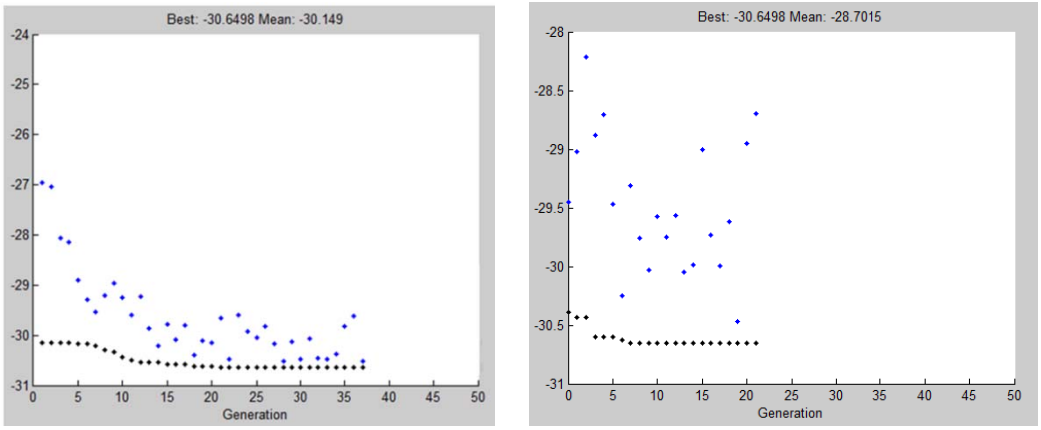

(a) (b)

Figure 2. Convergence Graphs for (a) GA and (b) EGA for real brain image (=15)

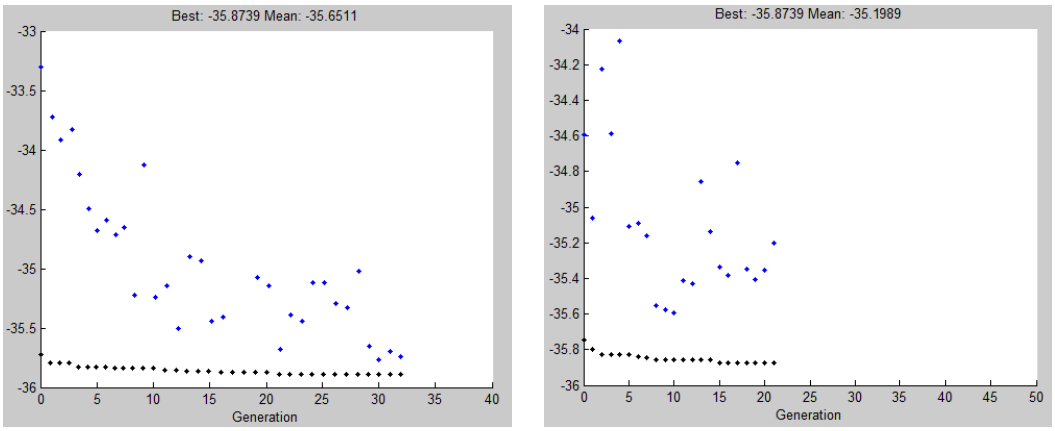

(a) (b)

Figure 3. Convergence Graphs for (a) GA and (b) EGA for synthetic brain image (=10)